C9orf72 deficiency promotes microglial mediated synaptic loss in aging and amyloid accumulation

Deepti Lall, Ileana Lorenzini, Thomas A. Mota , Shaughn Bell, Thomas E. Mahan, Jason D. Ulrich, Hayk Davtyan, Jessica E. Rexach, A.K.M. Ghulam Muhammad, Oksana Shelest, Jesse Landeros, Michael Vazquez, Junwon Kim, Layla Ghaffari, Jacqueline Gire O'Rourke, Daniel H. Geschwind, Mathew Blurton-Jones, David M. Holtzman, Rita Sattler, Robert H. Baloh

1. Figure S1: Related to Figure 1. Microglial profile in *C9orf72*$^{-/-}$ animals.

2. Figure S2: Related to Figure 1. Quality control of cells analyzed by scRNAseq and induction of interferon response genes in *C9orf72*$^{-/-}$ microglia.

3. Figure S3: Related to Figure 2. Lysosomal defects, microgliosis and loss of synaptic proteins in *C9orf72*$^{-/-}$ mice.

4. Figure S4: Related to Figure 5. Amyloid deposition, microglial reaction to plaques and neuronal quantification in 5XFAD/*C9orf72*$^{-/-}$ mice.

5. Figure S5: Related to Figure 5. Plaque associated Aβ-binding antibodies in 5XFAD/*C9orf72*$^{-/-}$ mice.

6. Figure S6: Related to Figure 6. CD68 positive accumulations and loss of synaptic proteins in 4-month old 5XFAD/*C9orf72*$^{-/-}$ mice.

7. Supplemental table S1 (excel file): Related to Figure 1 and Figure S2: QC data of scRNAseq dataset showing total number of cells sequenced per genotype, average reads per sample, median genes per cell and other cell types identified in analyses.

8. Supplemental table S2 (excel file): Related to Figure 1: QC data of all microglial clusters identified with scRNAseq and list of genes identified in each microglial cluster.

A

Microglia

BMDM

50KDa

C9orf72+/+ *C9orf72+/-* *C9orf72-/-*

C9orf72+/+ *C9orf72+/-* *C9orf72-/-*

C9orf72

42KDa

Actin

5μg sample per lane

B

Mean Intensity (A.U)

2000

1500

1000

500

0

- *C9orf72+/+* microglia
- *C9orf72+/-* microglia
- *C9orf72-/-* microglia
- *C9orf72+/+* BMDM
- *C9orf72+/-* BMDM
- *C9orf72-/-* BMDM

C

35172900 35173100 35173300 35173500

Neuron 2   68.40 0

Neuron 1   32.26 0

Microglia 2   60.50 0

Microglia 1   101.19 0

qA5
chr4

1b 1a

D

35173000 35173200 35173400 35173600

Astrocyte   32.68 0 32.26 0

Neuron

OPC   49.19 0

NFO   59.15 0

MO   24.97 0

Microglia 1   60.50 0

Microglia 2   101.19 0

qA5
chr4

1b 1a

E

3 month microglia Module Eigengene

0.6

0.4

0.2

0

-0.2

-0.4

*

C9orf72+/+ *C9orf72+/-* *C9orf72-/-*

17 month microglia Module Eigengene

0.4

0.2

0

-0.2

-0.4

* *

C9orf72+/+ *C9orf72+/-* *C9orf72-/-*

F

ICAM1, ITGAX, Ctss, CD74, Plau, Plaur, CD14, Gng5, CD180, Ly86, Gng2, Gng10, Fgr, Cebpb, Cybb, Tyrobp, CD22, Ptpn6, Ncf2, B2M, Il2rg, Cebpa, Trem2, Socs3, Fcer1g, Cdk1, Rpl23, Il1m, Ccl3, Rpl21, Il1b, Cxcl16, Cxcr4, Ccl4, Rpl18a, Pycard, Cxcl13

G

Homeostatic genes

row min — row max

P2ry12, Ccr5, Cd33, Csf1r, Cx3cr1, Glul, Gpr34, Adgrg1, Tgfb1, Tgfbr1, Serinc3, Siglech, Mertk, Bin1, Tmem119, Sall1, Mafb, Smad3, Mef2a, Egr1

H

Activated response genes

row min — row max

Lpl, Cst7, ApoE, Spp1, Itgax, Clec7a, Csf1, Igf1, Axl, Ccl6, Ctsz, Cd9, Trem2, Tyrobp, Ctsl, Cd63, Ank, Ctsd

I

Interferon response genes

row min — row max

Ifit1, Ifit3, Oas1a, Oas1g, Oas3, Oasl1, Oasl2, Isg15, Isg20, Irf7, Ly6a, Usp18, Ifitm2, Ifitm3, Csprs, Ccrl2, Stat2, Dhx58, Ifi27l2a, Ifit2, Ifit3

Figure S1: **Related to Figure 1. Microglial profile in *C9orf72$^{-/-}$* animals. (A)** Western blot of microglia and bone marrow derived macrophage (BMDM) lysates from *C9orf72$^{+/+}$*, *C9orf72$^{+/-}$*, and *C9orf72$^{-/-}$* animals (n=2 per genotype). **(B)** Quantification of western blot. **(C)** Representation of mapped RNAseq reads corresponding to mouse *C9orf72* exon 1a and 1b from isolated neurons, microglia, astrocytes, oligodendrocyte precursor cells (OPCs), newly formed oligodendrocytes (NFOs), mature oligodendrocytes (MOs), and endothelial cells (Zhang et al., 2014). Red box indicates reads from exon 1a, and green box exon 1b. **(D)** Single representative cells from each group showing mapped reads from individual cell types. **(E)** Eigengene of the preserved module from WGCNA analysis of 3 and 17-month-old *C9orf72$^{+/+}$* (grey), *C9orf72$^{+/-}$* (yellow) and *C9orf72$^{-/-}$* (magenta) mice. *p-value = 0.029 vs *C9orf72$^{+/+}$*, Wilcox Test. **(F)** Protein-protein interactions among the up-regulated inflammatory module using the STRING database. Each node represents all the proteins produced by a single, protein-coding gene locus. Colored nodes denote query proteins and first shell of interactors. Edges represent protein-protein associations. Lines denote edge confidence (thinnest-lowest, thickest-strongest). Heat maps of gene expression for genes representing **(G)** Homeostatic microglia, **(H)** Activated Response Microglia, and **(I)** Interferon Response Microglia from RNAseq of isolated microglia from *C9orf72$^{+/+}$* and *C9orf72$^{-/-}$* mice at 3 and 17-month. Gene lists from (Keren-Shaul et al., 2017; Krasemann et al., 2017; Sala Frigerio et al., 2019).

A Pre-harmony / Post-harmony: Batch, Order, Sex, Genotype

B
UMAP_2 vs UMAP_1 — Astrocytes, Neutrophils, Granulocytes, Microglia, Lymphocytes, Monocytes/Macrophages, Endothelial cells

C
Astrocyte — S100β
Endothelial cells — Cdh5
Monocyte/Macrophage — Cd163
Neutrophils — Ly6g

D
Percentage of cells

- *C9orf72⁺/⁺*
- *C9orf72⁺/⁻*
- *C9orf72⁻/⁻*

Microglia, Astrocytes, Monocytes/Macrophages, Endothelial, Granulocytes, Neutrophils, Lymphocytes

E
Tmem119   P2ry12   Trem2

F
Module score ARM cluster

Module score IRM cluster

G Activated response microglia
C9orf72⁺/⁺ *C9orf72⁺/⁻* *C9orf72⁻/⁻*

H Interferon response microglia
C9orf72⁺/⁺ *C9orf72⁺/⁻* *C9orf72⁻/⁻*

Figure S2: **Related to Figure 1. Quality control of cells analyzed by scRNAseq and induction of interferon response genes in *C9orf72$^{-/-}$* microglia. (A)** Representative images of UMAP plots before and after integration using HARMONY and correcting for process day, process order, and sex. **(B**) UMAP of different cell types that were identified with single-cell analysis and excluded from downstream microglia data analysis. **(C)** Representative violin plots of genes specific to a cell type within different contaminating cell clusters. S100β (Astrocytes), Cdh5 (endothelial cells), Cd163 (Monocytes/ Macrophages), Ly6g (Neutrophils). Minimum three genes were used to define specific cell type. **(D)** Plot of percentage of different cell types from different genotypes. **(E)** UMAP plot colored for expression of canonical microglial genes. **(F)** Module score for ARM and IRM clusters. **(G)** Heat map of top 30 positively differentially expressed genes in ARM cluster in *C9orf72$^{+/+}$*, *C9orf72$^{+/-}$* and *C9orf72$^{-/-}$* mice. **(H)** Heat map of top 30 positively differentially expressed genes in IRM cluster in *C9orf72$^{+/+}$*, *C9orf72$^{+/-}$* and *C9orf72$^{-/-}$* animals.
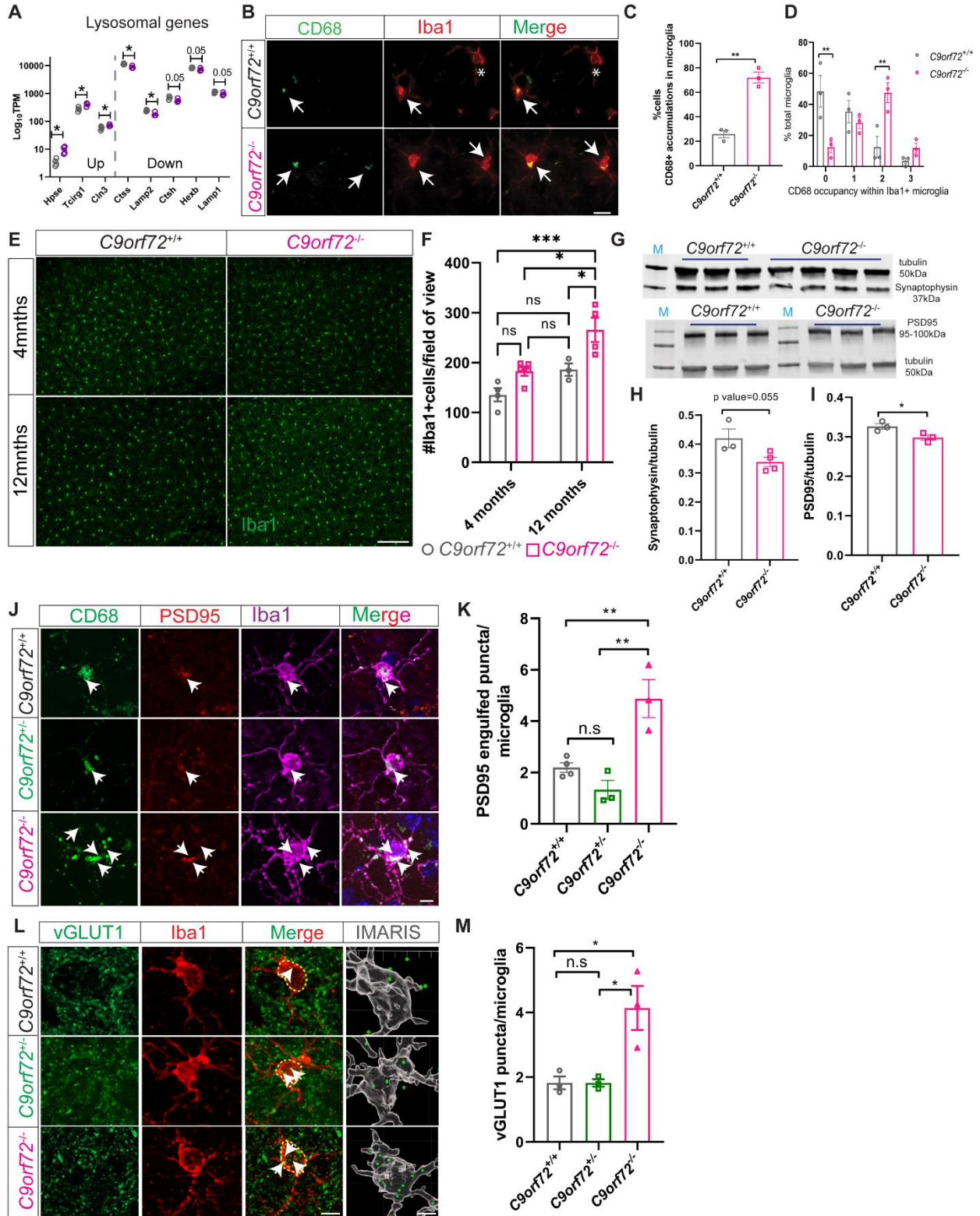
A Lysosomal genes

B CD68 | Iba1 | Merge

C %cells CD68+ accumulations in microglia

D CD68 occupancy within Iba1+ microglia

E C9orf72+/+ | C9orf72−/−

F #Iba1+cells/field of view

G M | C9orf72+/+ | C9orf72−/−

H Synaptophysin/tubulin

I PSD95/tubulin

J CD68 | PSD95 | Iba1 | Merge

K PSD95 engulfed puncta/microglia

L vGLUT1 | Iba1 | Merge | IMARIS

M vGLUT1 puncta/microglia

Figure S3: **Related to Figure 2. Lysosomal defects, microgliosis and loss of synaptic proteins in** *C9orf72*$^{-/-}$ **mice. (A)** TPM graph of up and downregulated lysosomal genes in 17-month old *C9orf72*$^{-/-}$ microglia. **(B)** Iba1 and CD68 co-stain in motor cortex of 17-month *C9orf72*$^{+/+}$ and *C9orf72*$^{-/-}$ mice showing CD68+ lysosomal accumulations (white arrows). * depicts microglia without any accumulation. 20-30 microglia per animal, mean ±SEM, unpaired t test, two-tailed, n=3 per genotype, **p=.0010. Scale bars: 20µm**. (C)** & **(D)** Quantification of cells with CD68+ lysosomal accumulations. **(E)** Immunostains for Iba1 in motor cortex from coronal sections of 4 and 12-month-old *C9orf72*$^{+/+}$ and *C9orf72*$^{-/-}$ mice. Scale bars: 100µm. **(F)** Quantification of microglial density in motor cortex of 4 and 12-month-old *C9orf72*$^{+/+}$ and *C9orf72*$^{-/-}$ mice, mean ±SEM, Two-way ANOVA with Sidak's multiple comparison test, n=3-5 per genotype per age, *p < 0.05, ***p < 0.005. **(G)** Representative western blots of synaptic markers in the cortex of 12-month *C9orf72*$^{+/+}$ and *C9orf72*$^{-/-}$ mice. **(H)** Relative quantification of synaptophysin and **(I)** PSD95 normalized to tubulin reference gene, mean ±SEM, Unpaired t-test, two-tailed, n=3-4 per genotype, *p<0.05. **(J)** Confocal images showing PSD95+ puncta (red) inside CD68+ vesicles (green) in Iba1+ microglia (purple) from 12-month old *C9orf72*$^{+/+}$, *C9orf72*$^{+/-}$, and *C9orf72*$^{-/-}$ mice. Scale bars: 5µm**. (K)** Quantification of PSD95 within Iba1+ microglia, mean ±SEM, n=3-4 per genotype, One-way ANOVA with Tukey's multiple comparison test, **p<0.005. **(L)** Representative images of vGLUT1+ puncta (green) inside Iba1+ microglia (red) in the motor cortex of 12-month *C9orf72*$^{+/+}$, *C9orf72/*$^{+-}$, and *C9orf72*$^{-/-}$ mice. Scale bars: 5µm**. (M)** Quantification of vGLUT1+ puncta per Iba1+ microglia, mean ±SEM, n=3 per genotype, One-way ANOVA with Tukey's multiple comparison test, *p<0.05.
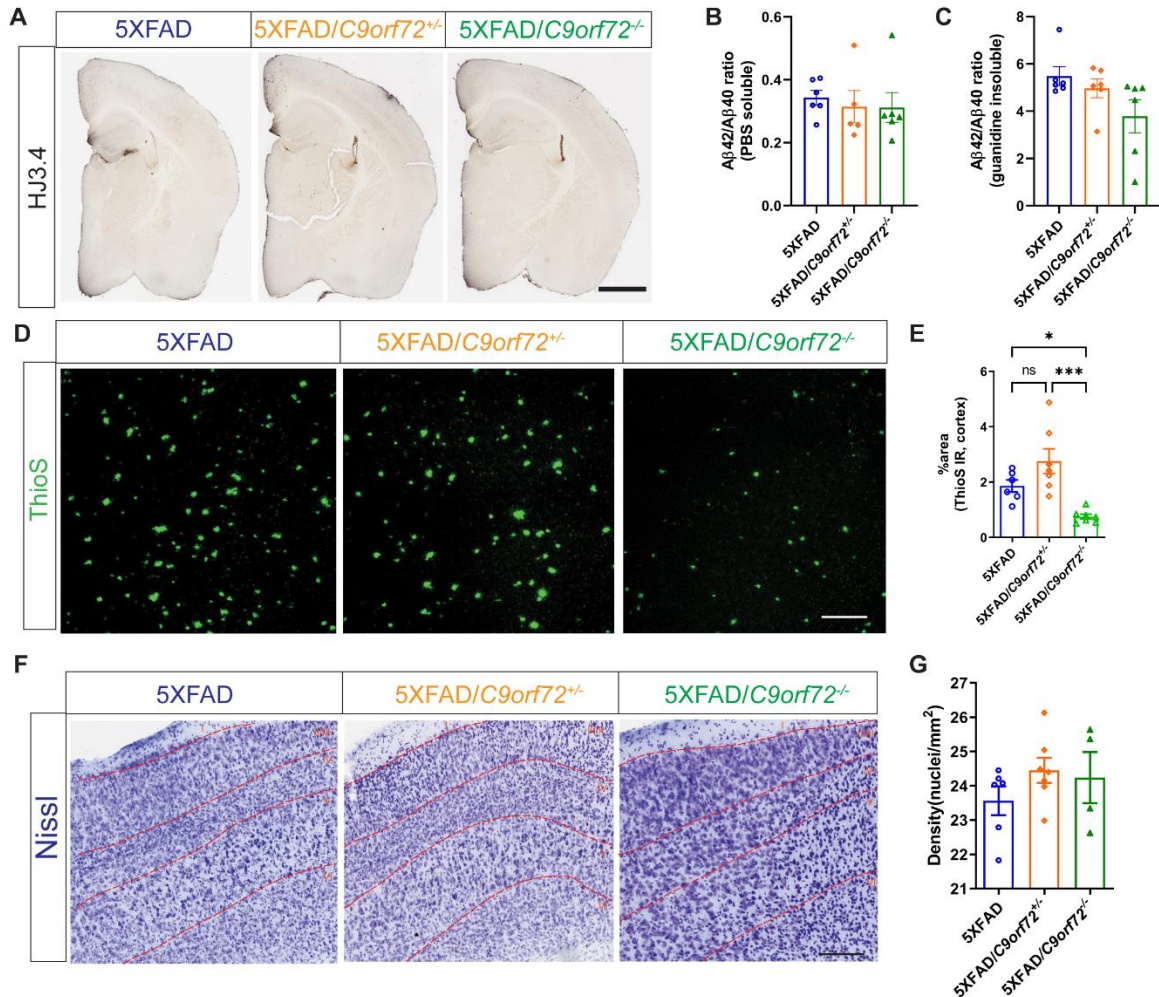
Figure S4: Related to Figure 5. Amyloid deposition, microglial reaction to plaques and neuronal quantification in 5XFAD/*C9orf72*^{-/-} mice. (A) mHJ3.4-stained matched coronal sections from 5XFAD, 5XFAD/*C9orf72*^{+/-}, and 5XFAD/*C9orf72*^{-/-} animals at 3 months showing no accumulation of amyloid in any genotype at this age. Scale bars: 100μm. **(B)** & **(C)** PBS soluble and guanidine insoluble Aβ42/Aβ40 ratio in 2-month old 5XFAD, 5XFAD/*C9orf72*^{+/-}, and 5XFAD/*C9orf72*^{-/-} animals, n=5-6 per genotype. **(D)**. ThioS immunoreactivity in the cortex of 6-month-old 5XFAD, 5XFAD/*C9orf72*^{+/-}, and 5XFAD/*C9orf72*^{-/-} mice. Scale bars: 100μm. **(E)** Quantification of ThioS immunoreactivity, n=6-7 per genotype, mean ±SEM, One-way ANOVA with Tukey's multiple comparison test, *p<0.05, ***p<0.0005. **(F)** Representative images of Nissl staining in the motor cortex of 6-month-old 5XFAD, 5XFAD/*C9orf72*^{+/-}, and 5XFAD/*C9orf72*^{-/-}

mice. Scale bars: 100μm. **(G)** Quantification of neuronal density in motor cortex, n=4-7 per
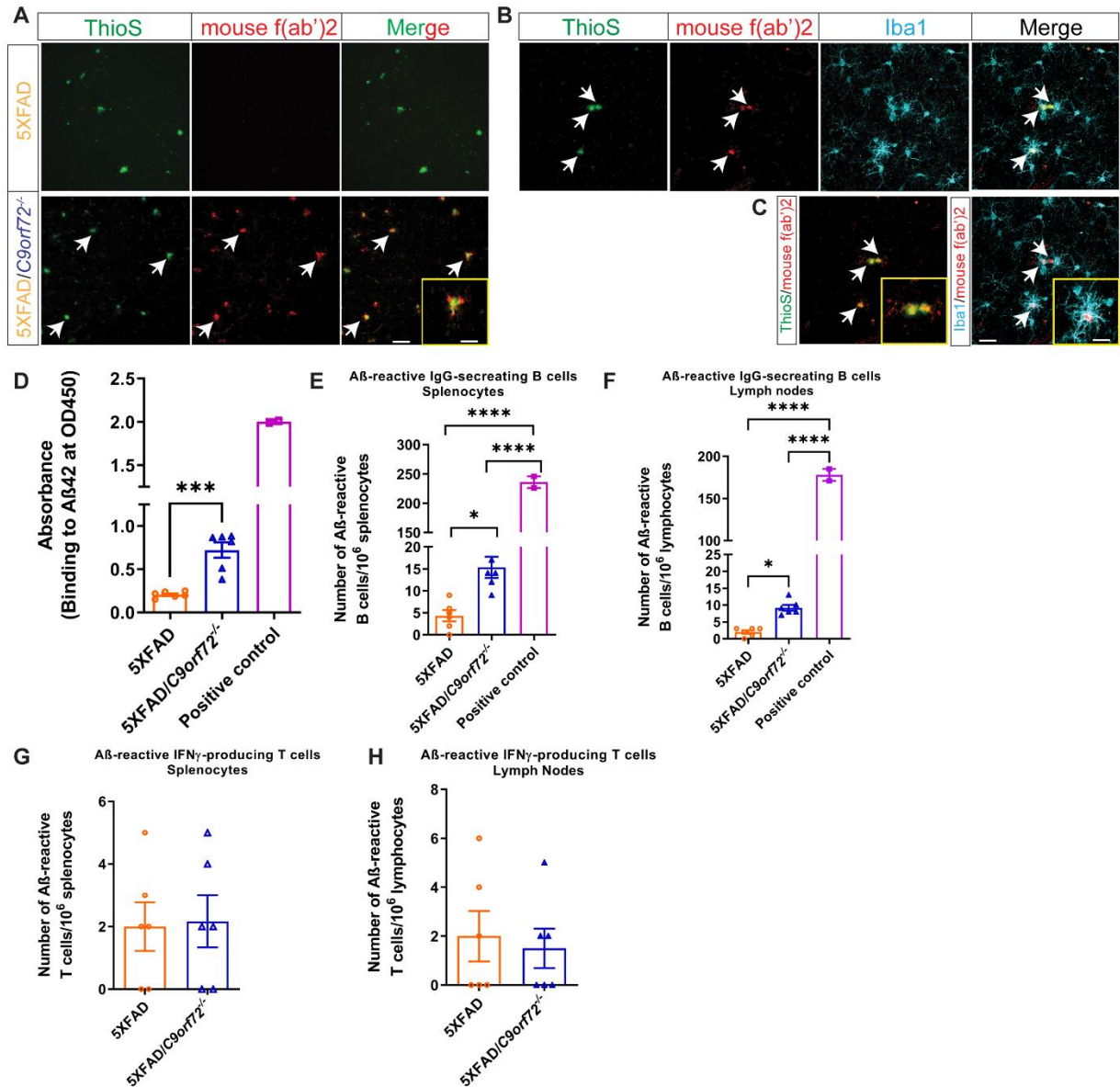
genotype, mean ±SEM.

Figure S5: Related to Figure 5. Plaque associated Aβ-binding antibodies in

5XFAD/*C9orf72*^-/- mice. (A) Representative confocal images showing mouse IgG (red) in close

association with ThioS+ plaques (green) in the brains of 6-month old 5XFAD/*C9orf72*^-/- but not in

5XFAD, animals. White arrows indicate co-labelling of IgG and plaques. Scale bars: 25μm, inset

10 μm. **(B)** Confocal maximum intensity projections showing increased levels of mouse IgG

(red) near microglial membranes (cyan) in the brains of 5XFAD/*C9orf72*^-/- mice. White arrows

indicate co-localization of Iba1+ microglia, IgG, and Thios+ plaques (green). **(C)** High

magnification confocal images further demonstrate co-labelling of Iba+ microglial processes with mouse IgG. Scale bars: 25µm, inset 10 µm. **(D)** ELISA of sera collected from 5XFAD and 5XFAD/*C9orf72*$^{-/-}$ mice at 6 months demonstrates elevated levels of Aβ-binding antibodies in 5XFAD/*C9orf72*$^{-/-}$ mice, mean ±SEM, n=6 per genotype, One-way ANOVA with Tukey's multiple comparison test, ***p<0.0005 **(E)** & **(F)** Aβ-binding B cells in 5XFAD/*C9orf72*$^{-/-}$ animals determined using ELISpot assay of splenocytes and lymphocytes (pooled deep and superficial lymph nodes). n=6 per genotype, mean ±SEM, One-way ANOVA with Tukey's multiple comparison test, *p<0.05, ****p<0.0001. **(G)** Number of reactive T cells in splenocytes or **(H)** lymphocytes were same across genotypes.
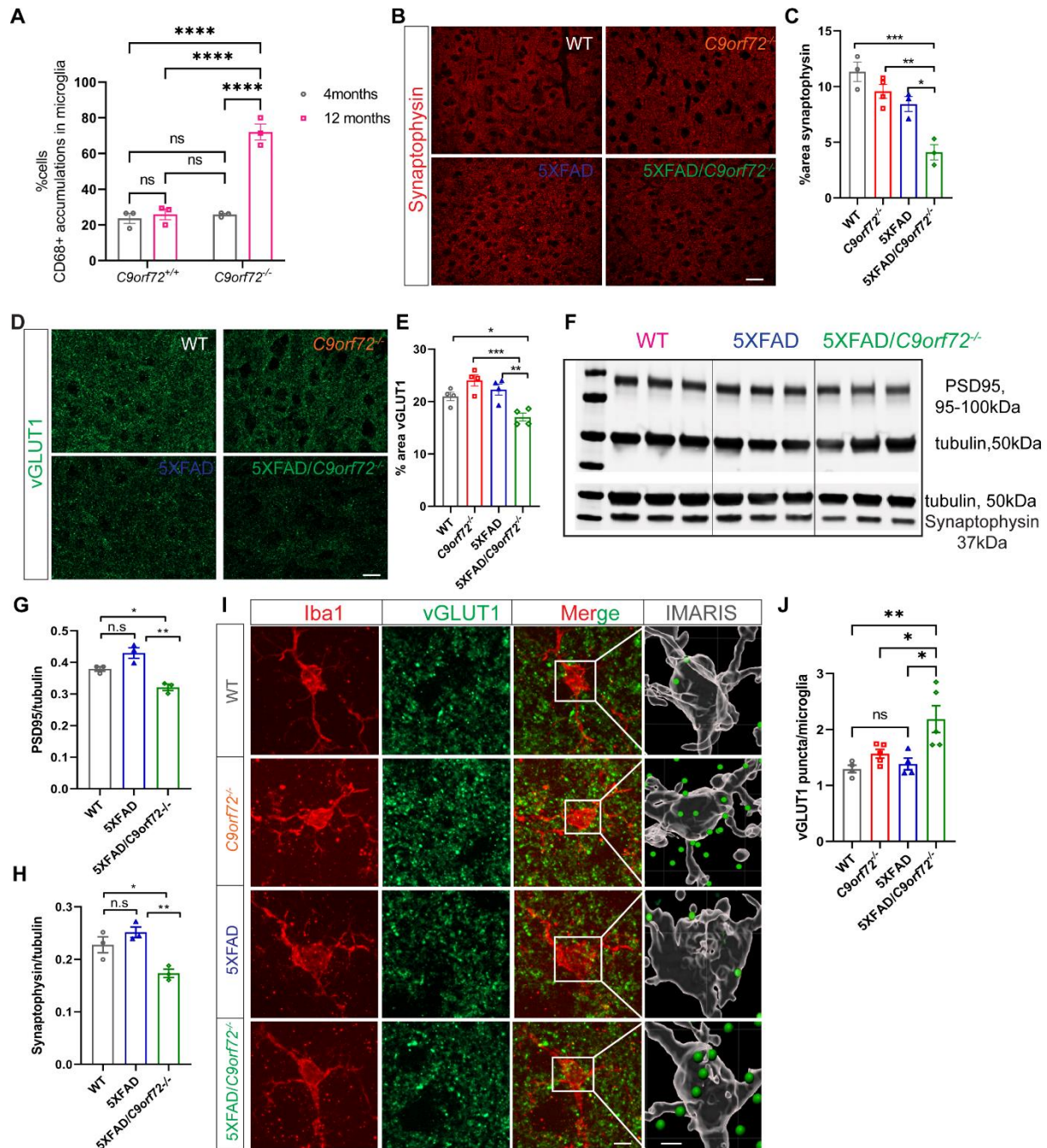
Figure S6: **Related to Figure 6. CD68 positive accumulations and loss of synaptic proteins in 4-month old 5XFAD/*C9orf72*^{-/-} mice. (A)** Quantification of percentage of cells showing CD68+ accumulations in microglia from *C9orf72*^{+/+} and *C9orf72*^{-/-} mice at 4 and 12 months. n=3 per genotype, mean ±SEM, Two-way ANOVA with Sidak's multiple comparison test, ****p<0.0001. **(B)** Representative confocal images of synaptophysin immunoreactivity, cale

bars 20µm and **(C)** quantification in 4-month old WT, *C9orf72*$^{-/-}$, 5XFAD, and 5XFAD/*C9orf72*$^{-/-}$ mice, n=3-4 per genotype, mean ±SEM, One-way ANOVA with Tukey's multiple comparison test, *p<0.05, **p<0.005, ***p<0.0005. **(D)** Confocal images of vGLUT1 immunoreactivity, scale bars 10 µm and **(E)** quantification in 4-month old WT, *C9orf72*$^{-/-}$, 5XFAD, and 5XFAD/*C9orf72*$^{-/-}$ mice, n=4 per genotype, mean ±SEM, One-way ANOVA with Tukey's multiple comparison test, *p<0.05, **p<0.005, ***p<0.0005. **(F)** Representative western blots of synaptic markers in the motor cortex of 4-month old WT, 5XFAD, and 5XFAD/*C9orf72*$^{-/-}$ mice. Relative quantification of **(G)** PSD95 and **(H)** synaptophysin normalized to tubulin reference gene, mean ±SEM, One-way ANOVA with Tukey's multiple comparison test, n=3 per genotype, *p=.0315, **p= .0016 for PSD95, *p=.0360, **p= .0070 for synaptophysin graphs. **(I)** Confocal and IMARIS reconstruction images showing vGLUT1+ puncta within Iba+ microglia in motor cortex of 4-month old WT, *C9orf72*$^{-/-}$, 5XFAD, and 5XFAD/*C9orf72*$^{-/-}$ mice. Scale bars: 5µm, IMARIS 1µm. **(J)** Quantification of vGLUT1+ within Iba1+ microglia, mean ±SEM, One-way ANOVA with Tukey's multiple comparison test, *p<0.05, **p<0.005.